(11) R. Segal, P. Shatkovsky, and I. Milo-Goldzweig, *Biochem. Pharmacol.*, **23**, 973 (1974).
(12) R. Segal and I. Milo-Goldzweig, *ibid.*, **24**, 77 (1975).
(13) R. Segal and E. Schlosser, *Arch. Microbiol.*, **104**, 147 (1975).
(14) R. B. Bosmann, *J. Membr. Biol.*, **4**, 113 (1971).
(15) W. Schmid, in "Modern Methods of Plant Analysis," vol. 3, K. Peach and M. V. Tracey, Eds., Springer, Berlin, Germany, 1955, p. 549.
(16) W. Wildebrandt, *Arch. Exp. Pathol. Pharmacol.*, **212**, 9 (1950).
(17) P. G. Lefevere, *Symp. Soc. Exp. Biol. Med.*, **8**, 118 (1954).
(18) W. Koenigs and E. Knorr, *Sitzungber. Bayr. Akad. Wiss.*, **30**, 103 (1900).
(19) W. Koenigs and E. Knorr, *Chem. Ber.*, **34**, 957 (1901).
(20) P. L. Durrete and D. Horton, *Adv. Carbohydr. Chem. Biochem.*, **26**, 49 (1971).
(21) G. Wulff, G. Rhole, and W. Kruger, *Chem. Ber.*, **105**, 1097 (1972).
(22) G. Zemplen and E. Pacsu, *ibid.*, **62**, 1613 (1929).
(23) G. Wulff and G. Rhole, *Angew. Chem. (Int. Ed.)*, **13**, 157 (1974).
(24) W. Klyne, *Biochem. J.*, **47**, XLI (1950).
(25) B. Iselin and T. Reichstein, *Helv. Chim. Acta*, **29**, 508 (1946).
(26) R. E. Reeves, *J. Am. Chem. Soc.*, **76**, 4595 (1954).
(27) R. Segal, M. Mansour, and D. V. Zaitschek, *Biochem. Pharmacol.*, **15**, 1411 (1966).
(28) R. Segal and I. Milo-Goldzweig, *ibid.*, **20**, 2163 (1971).
(29) R. Tschesche and G. Wulff, *Planta Med.*, **12**, 272 (1964).
(30) S. Shany, A. W. Bernheimer, P. S. Grushoff, and K. S. Kim, *Mol. Cell. Biochem.*, **3**, 179 (1974).
(31) G. P. Ellis and J. Honeyman, in "Carbohydrate Chemistry," vol. 10, E. L. Hirst and A. G. Ross, Eds., Academic, New York, N.Y., 1955, p. 95.
(32) M. N. Wolform and A. Thompson, in "Methods in Carbohydrate Chemistry," vol. 1, R. H. Whistler and M. L. Wolform, Eds., Academic, New York, N.Y., 1955, p. 334.
(33) D. Horton and J. H. Lauterbach, *Carbohydr. Res.*, **43**, 9 (1975).
(34) R. E. Deriaz, W. B. Overend, M. Stacey, E. G. Teece, and L. F. Wiggins, *J. Chem. Soc.*, **1949**, 1879.
(35) A. M. Gakhokize, *J. Gen. Chem. (USSR)*, **18**, 60 (1948); through *Chem. Abstr.*, **42**, 4948i (1948).
(36) E. Fischer, *Chem. Ber.*, **44**, 1903 (1911).
(37) B. Helferich and W. Klein, *Justus Liebigs Ann. Chem.*, **450**, 219 (1928).
(38) R. Segal, I. Milo-Goldzweig, D. V. Zaitschek, and M. Noam, *Anal. Biochem.*, **84**, 78 (1978).

ACKNOWLEDGMENTS

Supported in part by a grant from the Joint Research Fund of the Hebrew University and Hadassah.

The authors thank Professor G. Wulff (University of Bonn, Federal Republic of Germany) for samples of monoglycosides and for valuable discussions.

Nonisothermal Aqueous Calorimetry: Computation of Process-Dependent Temperature Change and Aspects of Calorimeter Design

R. GARY HOLLENBECK *, GARNET E. PECK, and DANE O. KILDSIG ˣ

Received July 29, 1977, from the *Department of Industrial and Physical Pharmacy, School of Pharmacy and Pharmacal Sciences, Purdue University, West Lafayette, IN 47907.* Accepted for publication March 23, 1978. *Present address: School of Pharmacy, University of Maryland, Baltimore, MD 21201.

Abstract □ A general method for determining the process-dependent (intrinsic) temperature change in a nonisothermal calorimeter is presented. The nonisothermal approach to calorimetric investigations requires an estimate of the magnitude of the process independent (extrinsic) temperature change during the reaction period. The proposed method can be applied to any calorimeter whose output is a discrete or continuous temperature–time profile. It is based on a first-derivative transformation of the temperature–time profile and the partitioning of the observed temperature variation into two components: pure extrinsic variation, which occurs outside the reaction period, and the combined extrinsic and intrinsic effects during the reaction period. Close examination of the pure extrinsic variation was considered essential, since it provided the basis for identifying the form of a descriptive mathematical function consistent with the observed extrinsic behavior. Once a suitable function was selected, parameters for the equation were determined through a linear regression procedure. The resulting equation was used to predict the extrinsic variation within the reaction period. Subtraction of predicted extrinsic variation from the observed total variation and integration over the time course of the experiment provide an estimate of the process-dependent temperature change. The differential approach was examined for processes performed in a calorimeter of simple design. Aspects of calorimeter design and advantages of the proposed method of data analysis are discussed.

Keyphrases □ Calorimetry, nonisothermal—general method for determining process-dependent temperature change, aspects of calorimeter design □ Instrument design—nonisothermal calorimeter, general method for determining process-dependent temperature change

Immersional calorimetry is a remarkably versatile technique for investigation of the wetting of hydrophilic and hydrophobic solids (1). Some applications of this analytical method were reported (2–7); yet, in view of its utility, these applications are few and limited.

The information available from calorimetric investigations could be of value in the formulation and evaluation of pharmaceutical products. Implementation of this general experimental technique has proceeded slowly, primarily because of the apparent sophistication necessary in the equipment.

Aspects of calorimeter design and data analysis were included in a general review of calorimetry (8). This paper presents a general method of data analysis and demonstrates its rational development for a calorimeter of simple design.

0022-3549/78/1100-1592$01.00/0

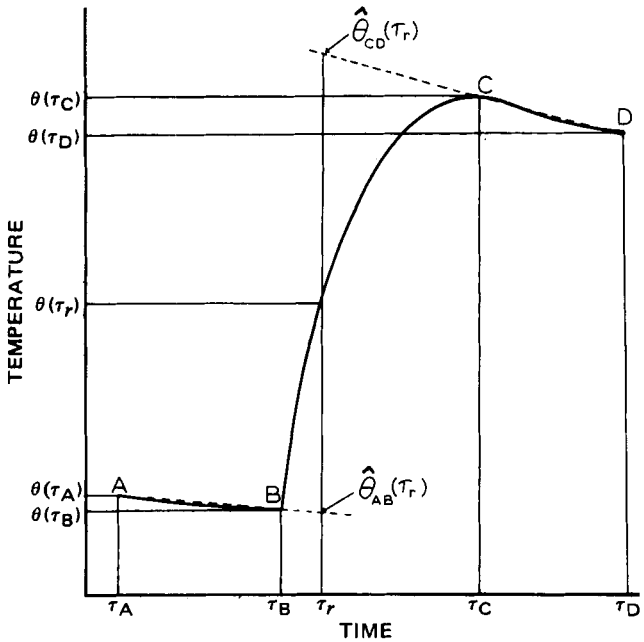

Figure 1—*Typical temperature–time profile for an exothermic process.*

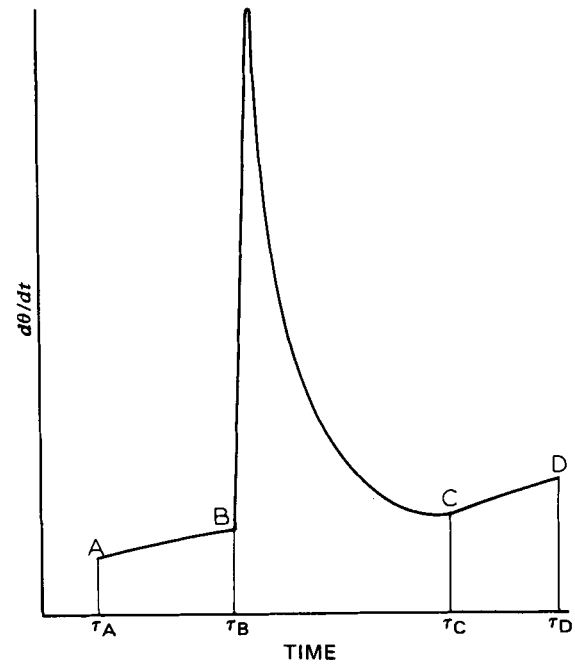

Figure 2—*First-derivative transformation of Fig. 1.*

THEORETICAL

Background—Equation 1 describes the basic relationship between the heat released by a process and the subsequent temperature change in a nonisothermal calorimeter:

$$-q = C\,\Delta\theta_i \qquad \text{(Eq. 1)}$$

where $-q$ is the heat released (calories), C is the heat capacity of the system (calories per degree celsius), and $\Delta\theta_i$ is the intrinsic temperature change (degrees celsius) in the calorimeter contents.

The term "intrinsic temperature change" refers to that portion of the total temperature change in the contents of the calorimeter that can be attributed to the process performed. Such a distinction is necessary, because it is not possible to insulate the reaction perfectly from its surroundings. In this manner, the total temperature change in the calorimeter contents, $\Delta\theta$, can be partitioned into two quantities:

$$\Delta\theta = \Delta\theta_i + \Delta\theta_e \qquad \text{(Eq. 2)}$$

where $\Delta\theta_e$ is the "extrinsic" or process-independent temperature change. The extrinsic change is primarily a consequence of heat lost or gained from the environment and of heat contributed by stirring.

Figure 1 depicts a typical temperature–time profile for a calorimetric investigation of an exothermic process, where point B represents the initiation of the process and point C is its completion. Periods A–B and C–D are often termed the initial and final rating periods, respectively, and correspond to extrinsic variation. In the ideal case of perfect insulation, the slope of these lines would be zero.

These periods are generally approximated by straight lines and the intrinsic temperature change determined by extrapolation of these lines through the reaction period BC:

$$\Delta\theta_i = \hat{\theta}_{CD}(\tau_r) - \hat{\theta}_{AB}(\tau_r) \qquad \text{(Eq. 3)}$$

where $\hat{\theta}_{CD}(\tau_r)$ and $\hat{\theta}_{AB}(\tau_r)$ refer to the temperature values at reference time τ_r obtained by linear extrapolation of the final and initial rating periods, respectively. This procedure is demonstrated graphically by the dashed lines in Fig. 1.

A frequently chosen reference point is the time when the actual system temperature, $\theta(\tau_r)$, is equal to the arithmetic mean of the temperature at points C and B:

$$\theta(\tau_r) = \frac{\theta(\tau_B) + \theta(\tau_C)}{2} \qquad \text{(Eq. 4)}$$

The method of rating period extrapolations, which is essentially empirical, can be used with acceptable accuracy for examination of a process with three characteristics: short duration, large intrinsic temperature change, and rating periods that can be expressed as linear functions of time.

A more sophisticated method of data analysis was developed in which the extrinsic temperature variation is characterized on theoretical grounds (8). This method is based on a modified form of Newton's law of cooling:

$$\frac{d\theta_e}{dt} = K[\theta_S - \theta(t)] + w \qquad \text{(Eq. 5)}$$

where $d\theta_e/dt$ is the extrinsic temperature variation, θ_S is the environmental temperature, $\theta(t)$ is the temperature of the calorimeter contents at time t, K is a proportionality constant termed the thermal leakage modulus, and w is another constant included to account for the effect of stirring.

If it is assumed that θ_S is known and constant, the parameters K and w can be obtained from the initial and final rating periods by employing a linear approximation in each period. The value of $\theta(t)$ is taken at the rating period midpoint, and $d\theta_e/dt$ is estimated by the slope of the line. A set of two simultaneous equations results from the substitution of corresponding values for $d\theta_e/dt$ and $\theta(t)$ into Eq. 5. These equations can be solved for K and w, so the extrinsic temperature change during the reaction period can be determined by integration of Eq. 5:

$$\Delta\theta_e = \int_{\tau_B}^{\tau_C} [K[\theta_S - \theta(t)] + w]\,dt \qquad \text{(Eq. 6)}$$

In explicit form, the expression for the intrinsic temperature change is obtained by expansion of Eq. 6 and substitution into Eq. 2:

$$\Delta\theta_i = \Delta\theta - \Delta\theta_e = \theta(\tau_C) - \theta(\tau_B) - (K\theta_S + w)(\tau_C - \tau_B) + K\int_{\tau_B}^{\tau_C} \theta(t)\,dt \qquad \text{(Eq. 7)}$$

Equation 7 represents an exact procedure for determining $\Delta\theta_i$ when Eq. 5 describes the extrinsic temperature variation of the system.

Because of the assumptions on which Eqs. 3 and 7 are based, neither is generally applicable to all data; nonlinearity with respect to time prohibits the use of Eq. 3, and nonlinearity with respect to temperature prohibits the use of Eq. 7.

The proposed method for the determination of the intrinsic temperature change is general and based solely on the observed extrinsic variation of the calorimeter.

Proposed Method for Computation of Intrinsic Temperature Changes—A series of steps can be taken to characterize explicitly the extrinsic temperature variation of a calorimeter and, thus, to determine the intrinsic temperature change on a rational basis.

Figure 2 represents the first-derivative transformation of the temperature–time profile presented in Fig. 1. As a result of this procedure, segments A–B and C–D comprise part of a "baseline," which represents the extrinsic variation. Substantial deviations from this baseline occur

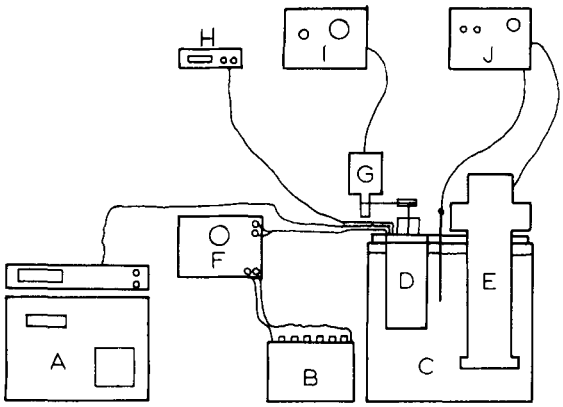

Figure 3—*Organizational schematic for components of the nonisothermal calorimeter. Key: A, digital quartz thermometer and digitial recorder; B, 12-v lead storage battery as dc power supply; C, environmental thermostat (insulated water reservoir covered with 1.9-cm acrylic); D, calorimeter cell; E, heating and water circulation unit; F, cell calibration control unit; G, stirring unit; H, digital voltmeter; I, control unit for stirrer; and J, control unit for constant-temperature water bath.*

in the reaction period B–C, and the observed $d\theta/dt$ values during this period represent the combination of intrinsic and extrinsic variations:

$$\frac{d\theta}{dt} = \frac{d\theta_i}{dt} + \frac{d\theta_e}{dt} \qquad \text{(Eq. 8)}$$

where $d\theta_i/dt$ is the intrinsic variation.

When the extrinsic temperature variation can be represented by a function capable of predicting its values *during* the reaction period, Eq. 8 may be rearranged and solved for $\Delta\theta_i$:

$$\Delta\theta_i = \int_{\tau_B}^{\tau_C} \left(\frac{d\theta}{dt} - g_e\right) dt \qquad \text{(Eq. 9)}$$

where g_e represents the function used to generate values of $d\theta_e/dt$.

The form of the function g_e should be elucidated from actual experimental data. Equation 5 is one form that may be suitable. This equation essentially states that the extrinsic variation is a first-order function of temperature:

$$\frac{d\theta_e}{dt} = g_e[\theta(t)] = B_0 + B_1\theta(t) \qquad \text{(Eq. 10)}$$

where $B_0 = K\theta_S + w$ and $B_1 = -K$. Substitution of Eq. 10 into Eq. 9, followed by integration between the limits of the reaction period, results in Eq. 7.

This linear form for g_e should only be used when the extrinsic variation is a linear function of temperature. Equation 11 represents a first-order function of time and temperature that was found to be more satisfactory than Eq. 5 for the calorimeter employed in this study:

$$\frac{d\theta_e}{dt} = B_0 + B_1 t + B_2\theta(t) \qquad \text{(Eq. 11)}$$

Parameters for either Eq. 10 or 11 can be obtained through a least-squares linear regression analysis based on the transformed data in periods A–B and C–D. Once these parameters are established, the solution of Eq. 9 is straightforward.

EXPERIMENTAL

Calorimeter—A nonisothermal calorimeter was designed and constructed to investigate immersional processes in water. Figure 3 represents the organization of the various components. The temperature recording device, A, and the calorimeter cell, D, are the primary components. Remaining components contribute partially or totally to one of three auxiliary functions: maintenance of constant environmental temperature, steady and efficient stirring of the calorimeter cell contents, and calibration of the cell (heat capacity determination).

A detailed drawing of the calorimeter cell is presented in Fig. 4. This cell was designed to fit into the acrylic[1] cover of an insulated water bath (C in Fig. 3) maintained at 25.00 ± 0.05°.

[1] Plexiglas.

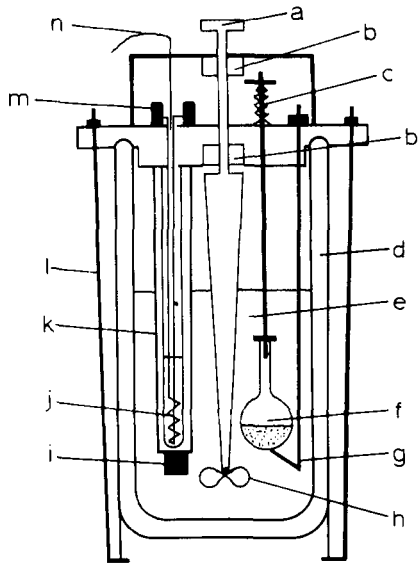

Figure 4—*Calorimeter cell. Key: a, belt guide for propeller drive shaft; b, ball bearing; c, spring-loaded sample bulb fracturing rod; d, insulated vessel; e, liquid (distilled water); f, thin-walled glass bulb containing sample; g, sample bulb support; h, propeller; i, quartz crystal thermometer probe; j, resistance heater; k, acrylic support; l, assembly rod; m, resistance heater leads; and n, thermometer lead.*

The temperature of the contents of the calorimeter cell was measured and recorded using a digital quartz thermometer[2] and output recorder[3]. With maximum resolution of 0.0001°, the output consisted of a concomitant temperature and time recording, which was updated at approximately 10-sec intervals. The quartz thermometer probe was affixed to a 16.0 × 1.5 × 0.32-cm acrylic[1] support (k in Fig. 4) within the calorimeter cell, which also served as a baffle and, thus, promoted mixing. Any thermal effect associated with the temperature measurement itself was assumed to be constant, contributing to and being characterized by the extrinsic variation.

Mounted on the opposite side of the acrylic support was a resistance heater for liquid temperature adjustment and determination of the cell heat capacity. This heater consisted of a section of wound nickel alloy[4] wire placed in a 10-mm diameter glass tube sealed at one end. Distilled water was added to cover the wire completely and to provide a medium for heat transfer. The leads from the heater were indirectly attached to a 12-v lead storage battery[5] (B in Fig. 3) through a calibration control unit (F in Fig. 3).

Within the cell, stirring was provided by an axially mounted propeller (h in Fig. 4) attached by a heavy gauge rubber band to the high revolutions per minute shaft of a commercially available stirring unit[6] (G in Fig. 3). A digital tachometer[7], based upon a photoelectric counter, was used to calibrate the stirrer. With a setting of 1500 rpm on the control unit, measurements throughout several experiments showed a tendency for the stirring rate to increase as time passed, starting at 1550 ± 25 rpm and eventually stabilizing at 1620 ± 5 rpm. The setting of 1500 rpm was used in all experiments.

The remaining components within the calorimeter cell comprise an assembly designed to contain the sample under investigation and to release it into the liquid at the appropriate time. A thin-walled glass bulb (f in Fig. 4), blown from 10-mm o.d. glass tubing, was used to contain the sample and isolated it from the immersion liquid. The bulb containing the sample was attached to an actuation rod (c in Fig. 4). Depression of the rod forced the sample bulb against a stationary support, resulting in fracture of the glass. After fracture, a spring mechanism returned the assembly to its original position so that the heat capacity of the cell was only slightly altered.

All components of the cell and all processes therein were isolated from

[2] Model 2801A, Hewlett-Packard, Palo Alto, CA 94303.
[3] Model 5050B, Hewlett-Packard, Palo Alto, CA 94303.
[4] Nichrome.
[5] Delco energizer E5000-R59, Delco Remy Division, General Motors Corp.
[6] Stedi-Speed stirrer, Fisher Scientific Co., Chicago, Ill.
[7] Designed by Professor G. Peck and Mr. T. McDaniels, Purdue University, West Lafayette, Ind.

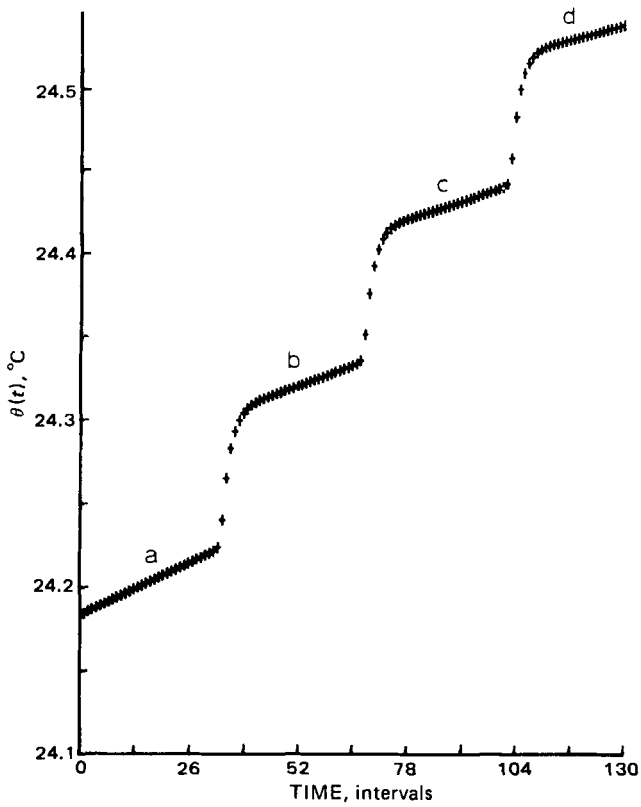

Figure 5—*Temperature–time profile for calibrations 1–3 in Table I. The periods a–d are the rating periods corresponding to the extrinsic temperature variation when the system temperature is below the environmental temperature.*

the environment by virtue of the Dewar flask (d in Fig. 4) in which they were contained. Unless otherwise specified, 250 ml of distilled water was placed in this flask and served as the immersional liquid.

Calibration—Calibration of the calorimeter consisted of a procedure used to determine the heat capacity of the cell. This procedure involved introducing a known amount of thermal energy into the cell and measuring the associated intrinsic temperature change. Completion of the circuit containing the resistance heater for a period of time, D, resulted in the release of a quantity of heat calculated from the following equation:

$$-q = V^2D/4.184R \qquad \text{(Eq. 12)}$$

where $-q$ is the heat released (calories), V is the voltage drop across the heater, and R is the resistance of the heater (ohms).

The calibration control unit (F in Fig. 3), which was directly attached to the power supply, was designed and manufactured to serve two purposes: voltage stabilization and heater activation. A center-off double-throw toggle switch was employed; when the switch was in the LOAD position, a circuit containing three 1-ohm resistors was completed. This circuit served as an external load to stabilize the power supply. When the switch was in the RUN position, the circuit containing the resistance heater was completed and, simultaneously, an elapsed time indicator[8] was actuated.

During actuation, the voltage across the terminals of the cell was measured using a digital voltmeter[9] with a resolution of 0.001 v. Movement of the control switch to the center-off position simultaneously opened the heater circuit and stopped the timer. The elapsed time was recorded with an accuracy of ±0.05 sec.

Also contained within the control unit was a 5-ohm variable resistor in series with the heater. Before a calibration was performed, the total resistance of this circuit was adjusted so that it equaled the resistance of the external load circuit. In this manner, movement of the control switch from the LOAD to RUN position did not result in a change in the potential drop across the power supply.

[8] Model 635K, Cramer/Cleveland, Cleveland, Ohio.
[9] Model 1450, Data Precision Corp., Wakefield, Me.

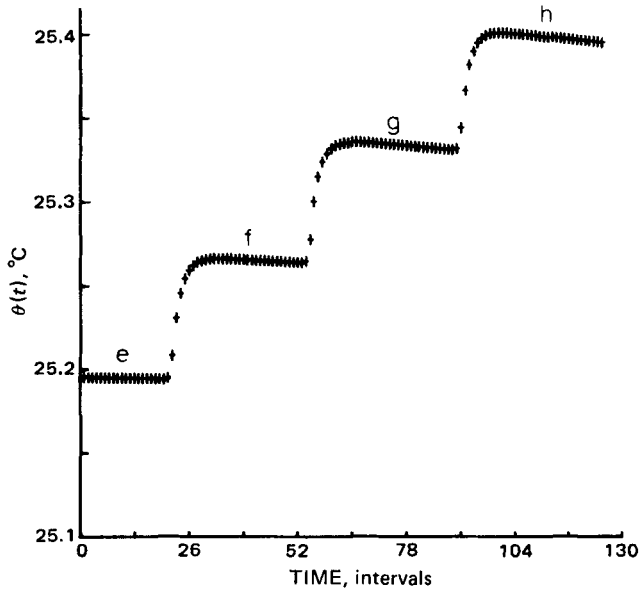

Figure 6—*Temperature–time profile for calibrations 4–6 in Table I. The periods e–h are the rating periods corresponding to the extrinsic temperature variation when the system temperature is above the environmental temperature.*

Solution of Eq. 12 for q requires a value for R, the resistance of the nickel alloy wire heater. This value is difficult to obtain by direct measurement, because the resistance is low and its value changes as the wire is heated. A retrogressive technique was employed to obtain an "effective" resistance for the heater. This technique consisted of performing a process of known magnitude in the calorimeter and comparing the temperature change induced in this manner with the intrinsic change associated with a calibration. The dissolution of coarse sodium chloride was examined, and Eqs. 1 and 12 were combined to give:

$$R' = \frac{V^2D\ \Delta\theta_{i(\text{soln})}}{q_{\text{soln}}\ \Delta\theta_{i(\text{calib})}} \qquad \text{(Eq. 13)}$$

where R' is the effective resistance, $\Delta\theta_{i(\text{soln})}$ is the intrinsic temperature change associated with dissolution, $q_{(\text{soln})}$ is the heat of solution of sodium chloride, and $\Delta\theta_{i(\text{calib})}$ is the intrinsic temperature change resulting from calibration.

A value of 0.475 ohm was obtained in this manner.

Examination of Temperature Effect on Extrinsic Variation—The applicability of Eq. 10 was tested by examining the extrinsic variation at several temperatures above and below the environmental temperature.

The calorimeter cell was filled with 250 ml of distilled water, cooled slightly to approximately 24°. After assembly of the calorimeter cell and placement in the constant-temperature water bath, stirring was initiated and 30 min was allowed for thermal stabilization. The thermometer was then turned on, and the temperature of the calorimeter contents was recorded with a resolution of 0.0001° at approximately 10-sec intervals.

The external load resistance was applied across the power supply for at least 5 min (30 intervals). After this voltage stabilization, the heater was actuated for approximately 10 sec, during which the voltage across the resistance was measured and recorded. When the heater was turned off, the duration of the heating process was recorded; sufficient time was allowed for stabilization of the extrinsic behavior. This heating procedure was repeated two more times.

After the third calibration was completed, the heater was actuated until the system temperature reached approximately 25°. The system also was altered by securing the sample bulb breaker rod in the depressed position. This action was taken to produce a significant change in the heat capacity of the calorimeter and, thus, to test the sensitivity of calibration.

When the system had stabilized, another three calibrations were subsequently performed at these higher temperatures. Thus, the calorimeter response and extrinsic temperature change were observed at temperatures both above and below the environmental temperature. Figures 5 and 6 show the temperature–time plots for the six processes. The extrinsic temperature change has a positive slope when the temperature is below that of the environment (Fig. 5) and a negative slope when the temperature is above that of the environment (Fig. 6).

Table I—Temperature–Time Output Data for the Investigation of the Wetting of Microcrystalline Cellulose

t[a]	$\theta(t)$	t[a]	$\theta(t)$
1	25.0094	50	25.0344
2	25.0093	51	25.0345
3	25.0093	52	25.0347
4	25.0092	53	25.0348
5	25.0092	54	25.0349
6	25.0092	55	25.0352
7	25.0091	56	25.0353
8	25.0092	57	25.0355
9	25.0091	58	25.0355
10	25.0092	59	25.0358
11	25.0091	60	25.0359
12	25.0091	61	25.0361
13	25.0091	62	25.0362
14	25.0092	63	25.0364
15	25.0093	64	25.0366
16	25.0092	65[b]	25.0373
17	25.0093	66[b]	25.0483
18	25.0094	67[b]	25.0676
19	25.0095	68[b]	25.0809
20	25.0095	69[b]	25.0894
21	25.0096	70[b]	25.0943
22	25.0096	71[b]	25.0976
23	25.0097	72[b]	25.0096
24	25.0099	73[b]	25.1008
25	25.0099	74[b]	25.1017
26	25.0100	75[b]	25.1024
27	25.0101	76[b]	24.1025
28	25.0102	77[b]	25.1028
29	25.0103	78[b]	25.1031
30	25.0104	79[b]	25.1032
31[c]	25.0251	80	25.1034
32[c]	25.0325	81	25.1035
33[c]	25.0326	82	25.1036
34	25.0326	83	25.1037
35	25.0327	84	25.1039
36	25.0327	85	25.1039
37	25.0329	86	25.1040
38	25.0329	87	25.1041
39	25.0330	88	25.1043
40	25.0331	89	25.1044
41	25.0333	90	25.1045
42	25.0334	91	25.1046
43	25.0335	92	25.1048
44	25.0336	93	25.1049
45	25.0338	94	25.1050
46	25.0339	95	25.1051
47	25.0340	96	25.1052
48	25.0342	97	25.1053
49	25.0342	98	25.1055

[a] Time expressed in intervals, where each interval is approximately 10 sec. [b] Time point included in calibration period where $V = 2.035$ v and $D = 10.10$ sec. [c] Time point included in reaction period.

Sample Process Investigation—The wetting of a sample of dried microcrystalline cellulose was examined to demonstrate the application of the differential method of process analysis and the validity of Eq. 11. An accurately weighed quantity of powder was placed in a glass sample bulb and attached to the breaker rod in the calorimeter cell. The cell was filled with 250 ml of distilled water and assembled. After stirring was initiated, 15 min of stabilization was allowed.

When the system appeared to be at thermal equilibrium, the temperature recording was started. After 5 min (30 intervals), the sample bulb was broken. Following another 5 min, during which the external load was applied across the storage battery, a calibration was performed.

Table I contains the thermometer output and calibration data from this experiment.

Data Transformation—The first derivative of the experimental data was approximated by finding the difference between successive temperature recordings. This approximation corresponds to the slope of the temperature–time profile, $\Delta\theta/\Delta t$, at the midpoint of each interval.

The actual data from the first calibration in Fig. 5 are given in Table II, where the transformation was explicitly performed. The entire data associated with Figs. 5 and 6 were transformed in this manner, and the resulting differential values are presented in Fig. 7. Transformed data from the sample wetting process are presented in Fig. 8.

These figures include only $\Delta\theta/\Delta t$ values less than 0.0020°.

Estimation of Parameters—The differential transformation (Figs. 7 and 8) provided a method for determining parameters of the function g_e. The points that should be identified with the reaction periods were clearly distinguished from those belonging to the rating periods. For example, in the first calibration (Table II), the $\Delta\theta/\Delta t$ values at times 1.5–31.5 and 44.5–64.5 were identified as belonging to rating periods a and b (Fig. 7), respectively. The $\Delta\theta/\Delta t$ values at times 32.5–43.5 were considered to be associated with the reaction period.

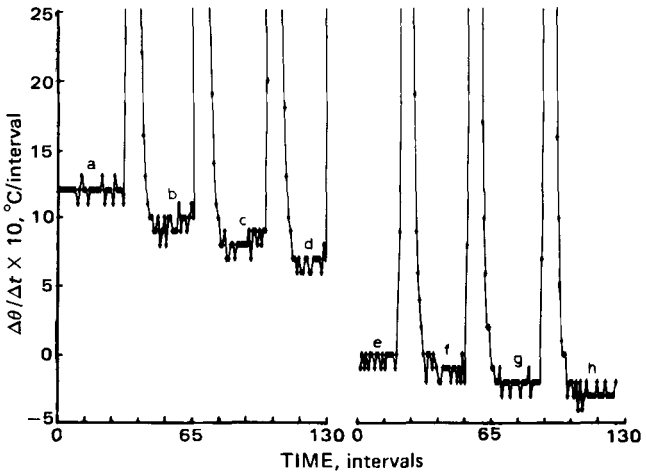

Figure 7—*Differential transformation of temperature–time profiles for calibrations 1–6 of Table I. The rating periods a–h with essentially constant $\Delta\theta/\Delta t$ values are easily distinguished from the reaction periods where these values are considerably greater in magnitude.*

Once identified as such, the entire rating period information from an experiment was used to estimate the parameters of the function g_e. For an investigation where Eq. 10 was employed as the descriptive equation for extrinsic variation, $[\Delta\theta/\Delta t, \theta(t)]$ coordinates from the rating periods were entered into a linear regression analysis to predict B_0 and B_1. When the form of Eq. 11 was employed for g_g, $[\Delta\theta/\Delta t, t, \theta(t)]$ values were entered into a multiple linear regression analysis to predict B_0, B_1, and B_2. In both cases, $\theta(t)$ was taken as the arithmetic mean interval temperature.

Computation of $\Delta\theta_i$—For computational purposes, Eq. 9 can be rewritten as:

$$\Delta\theta_i = \sum_{\substack{\text{reaction}\\ \text{period}}} \left(\frac{\Delta\theta}{\Delta t} - \frac{\Delta\hat{\theta}_e}{\Delta t}\right) \Delta t \qquad \text{(Eq. 14)}$$

where $\Delta\hat{\theta}_e/\Delta t$ is the predicted value of the extrinsic variation during the reaction at each successive time interval midpoint. These predicted values were obtained from the function g_e whose parameters were identified in the previous section. Equation 14 represents the sum of the residuals in the reaction period.

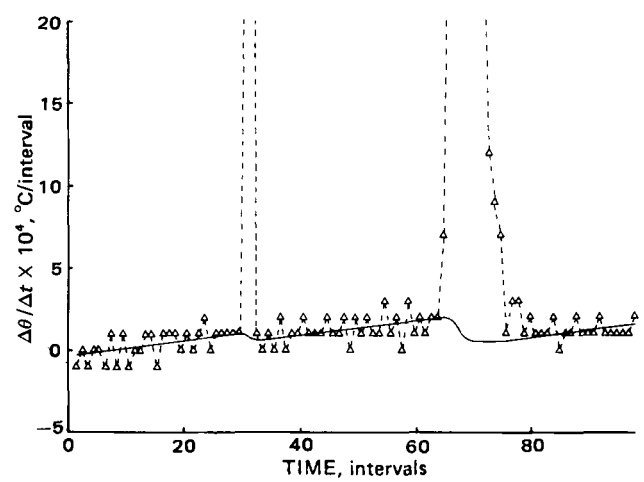

Figure 8—*Differential transformation of temperature–time data in Table II. Key: Δ, actual $\Delta\theta/\Delta t$ values; —, continuous prediction function, $\hat{g}_e$.*

Table II—Transformation of Thermometer Output for Calibration 1 of Fig. 5 and Predicted Extrinsic Variation

t, intervals	$\theta(t)$, °C	t, intervals	$\Delta\theta/\Delta t$, °C/interval	$\Delta\hat{\theta}_e/\Delta t$, °C/interval	t^b, intervals	$\theta(t)$, °C	t, intervals	$\Delta\theta/\Delta t$, °C/interval	$\Delta\hat{\theta}_e/\Delta t^a$, °C/interval
1	24.184	1.5	0.0012	0.00121	34	24.2403	34.5	0.0253	0.00111
2	24.1859	2.5	0.0012	0.00120	35	24.2656	35.5	0.0176	0.00107
3	24.1871	3.5	0.0012	0.00120	36	24.2832	36.5	0.0101	0.00105
4	24.1883	4.5	0.0012	0.00120	37	24.2933	37.5	0.0066	0.00104
5	24.1895	5.5	0.001	0.00120	38	24.2999	38.5	0.0042	0.00103
6	24.1907	6.5	0.0012	0.00120	39	24.3041	39.5	0.0027	0.00102
7	24.1919	7.5	0.0012	0.00120	40	24.3068	40.5	0.0022	0.00102
8	24.1931	8.5	0.0012	0.00119	41	24.3090	41.5	0.0016	0.00102
9	24.1943	9.5	0.0011	0.00119	42	24.3106	42.5	0.0013	0.00101
10	24.1954	10.5	0.0012	0.00119	43	24.3119	43.5	0.0011	0.00101
11	24.1966	11.5	0.0013	0.00119	44	24.3130	44.5	0.0010	0.00101
12	24.1979	12.5	0.0012	0.00119	45	24.3140	45.5	0.0010	0.00101
13	24.1991	13.5	0.0012	0.00119	46	24.3150	46.5	0.0009	0.00101
14	24.2003	14.5	0.0011	0.00118	47	24.3159	47.5	0.0009	0.00101
15	24.2014	15.5	0.0012	0.00118	48	24.3168	48.5	0.0010	0.00101
16	24.2026	16.5	0.0012	0.00118	49	24.3178	49.5	0.0008	0.00101
17	24.2038	17.5	0.0012	0.00118	50	24.3186	50.5	0.0009	0.00100
18	24.2040	18.5	0.0012	0.00118	51	24.3195	51.5	0.0010	0.00100
19	24.2062	19.5	0.0012	0.00118	52	24.3205	52.5	0.0008	0.00100
20	24.2074	20.5	0.0012	0.00117	53	24.3213	53.5	0.0010	0.00100
21	24.2086	21.5	0.0013	0.00117	54	24.3223	54.5	0.0010	0.00100
22	24.2099	22.5	0.0011	0.00117	55	24.3233	55.5	0.0009	0.00100
23	24.2110	23.5	0.0012	0.00117	56	24.3242	56.5	0.0009	0.00100
24	24.2122	24.5	0.0012	0.00117	57	24.3251	57.5	0.0009	0.00099
25	24.2134	25.5	0.0012	0.00116	58	24.3260	58.5	0.0011	0.00099
26	24.2146	26.5	0.0011	0.00116	59	24.3271	59.5	0.0009	0.00099
27	24.2157	27.5	0.0013	0.00116	60	24.3280	60.5	0.0010	0.00099
28	24.2170	28.5	0.0012	0.00116	61	24.3290	61.5	0.0010	0.00099
29	24.2182	29.5	0.0012	0.00116	62	24.3300	62.5	0.0009	0.00099
30	24.2194	30.5	0.0012	0.00116	63	24.3309	63.5	0.0010	0.00099
31	24.2206	31.5	0.0011	0.00115	64	24.3319	64.5	0.0011	0.00099
32	24.2217	32.5	0.0023	0.00115	65	24.330	65.5		
33	24.2240	33.5	0.0163	0.00114		24.3340			

[a] Predicted extrinsic temperature variation at interval midpoint. [b] One interval ≃ 10 sec.

RESULTS AND DISCUSSION

Examination of Extrinsic Variation—Examination of the differential curve in Fig. 7 indicated that temperature was an important independent variable for purposes of characterizing the extrinsic temperature variation. Figure 9 depicts this relationship over the combined temperature range of both calibration experiments. The $\Delta\theta_e/\Delta t$ values used in the construction of this figure were obtained by averaging the last 10 values in each rating period of Fig. 7. These estimates of $d\theta_e/dt$ were plotted at the final temperature in the period.

Over a relatively large temperature range (0.2°), Eq. 10 appeared to describe the data reasonably well. However, there was evidence that this form of g_e was not satisfactory during the rating period.

Solution of Eq. 10 in the time domain results in an expression containing an exponentially decreasing term. The absolute values of $d\theta_e/dt$ within any period should always decrease with time. This behavior clearly did not occur in Fig. 7 where $\Delta\theta_e/\Delta t$ values are quite constant. In periods b, c, and d, there actually appears to be an increasing trend.

The increasing trend in the rating periods is not obvious because of the short duration of these periods. It is somewhat more discernible in the extrinsic periods of Fig. 8. In fact, having established that temperature is an important independent variable, the extrinsic behavior in a typical experiment such as the one represented in Fig. 8 should be scrutinized. It is in this scrutiny that several fallacies of the generally employed methods of analysis can be recognized.

The method of rating period extrapolations is based upon the assumption that $d\theta_e/dt$ is a constant throughout the rating period. In Fig. 8, the values of $\Delta\theta_e/\Delta t$ tend to increase slightly in each period throughout the experiment, indicating that the temperature is not a first-order function of time alone.

A somewhat philosophical consequence of the actual nonlinearity of the extrinsic variation becomes important when the method of rating period extrapolations is employed. Assuming that the rating periods provide information about the nature of the system, it seems wise to collect as much information as possible, *i.e.*, to use a relatively long rating period. However, the more information obtained, the less acceptable is the linear hypothesis. The two extreme alternatives that arise from this contradiction are both unacceptable: extrapolation of a "poor" line based on a lot of information and extrapolation of a "good" line based on very little information. The acceptable linear fit obtained by using a short rating period should not be construed as a valid basis for extrapolation of the line over a relatively long reaction period.

A good general rule to follow when using this empirical method is to consider rating periods of a duration equal to or greater than the process itself. If the linear approximation is still reasonable, the method can be employed with negligible error.

The alternative method presented in the theoretical background sec-

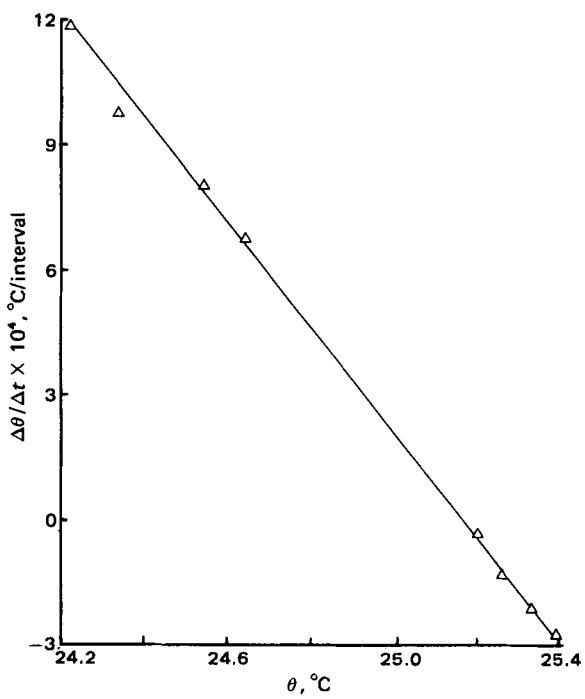

Figure 9—*Relationship between system temperature, θ, and extrinsic temperature variation, Δθ/Δt.*

Table III—Heat Capacity Values Determined from the Calibration Processes of Fig. 7 and Table II

Calibration	$-q$, cal	$\Delta\theta_i$, °C	C, cal/deg
1	21.732	0.07825	277.7
2	20.984	0.07563	277.4
3	21.046	0.07642	275.4
4	20.984	0.07145	293.7
5	20.860	0.07175	290.7
6	20.942	0.07143	293.2

tion represents an exact procedure when Eq. 10 describes the extrinsic variation; however, this method should not be used perfunctorily. The positive values for $d\theta_e/dt$ in Fig. 8 indicate a system whose temperature is below environmental temperatures. Therefore, any exothermic process should result in a postprocess rating period whose $d\theta/dt$ values are lower than the preprocess period. Both the wetting and calibration processes in Fig. 8 are exothermic, but neither reaction is followed by a decrease in $d\theta_e/dt$.

On the basis of these observations, the form used for g_e was that presented in Eq. 10: a function of time and temperature. The solid line in Fig. 8 was constructed from values generated through the following equation:

$$\frac{\Delta\hat{\theta}_e}{\Delta t} = 0.07509 - (4.9776 \times 10^{-6})t - (3.0042 \times 10^{-3})\theta(t) \quad \text{(Eq. 15)}$$

This equation was predicted using multiple least-squares regression based on $[\Delta\theta/\Delta t, t, \theta(t)]$ coordinates at time intervals 1.5–29.5, 33.5–63.5, and 80.5–97.5. The line appears to describe the experimental data, including the increasing trends within each period.

Table II also includes $\Delta\hat{\theta}_e/\Delta t$ values predicted from an equation of the form of Eq. 11 for the first calibration process of Figs. 5 and 7. These values compare well with the observed $\Delta\theta/\Delta t$ values in rating periods a and b.

There is no reason why an equation of the form of Eq. 11 cannot be used routinely. If either time or temperature proves to be negligible, the coefficients will reflect that fact.

Computation of $\Delta\theta_i$—Equation 14 was used to compute the intrinsic temperature changes associated with all processes investigated.

Table III contains the results of the six successive calibrations. The closeness of the heat capacity measurement in each set of determinations is reasonable considering the error associated with calculation of $-q$ from Eq. 12. Fixing the breaker rod in the depressed position resulted in a heat capacity increase of approximately 16 cal/°C.

For the wetting of the solid represented in Table I, intrinsic temperature changes of 0.02200 and 0.06546° were obtained for the wetting and calibration processes, respectively. A heat capacity of 321.15 cal/°C and a heat of wetting of −7.07 cal were obtained from these data.

SUMMARY AND CONCLUSIONS

Determination of the process-dependent temperature change in any nonisothermal calorimeter is predicated on a mathematical characterization of the process-independent or extrinsic temperature variation. With respect to the most frequently employed methods of data analysis, the following points should be emphasized:

1. The method of linear extrapolations is based, implicitly, on the assumption that the rating periods can be described by a function of time alone. When employing this method, the assumption should be critically tested by an examination of rating periods equal to or, preferably, greater in duration than the process itself.

2. More sophisticated methods are generally based on a form of Newton's law of cooling. When employing these methods, the actual extrinsic experimental behavior must be described adequately by a function of temperature alone.

The experiment presented can be used to assess the influence of temperature on the extrinsic variation of any calorimeter. Through an experiment of this type and a close investigation of a typical process, a rational decision can be made regarding the method used to compute the intrinsic change. In many cases, a conventional method is satisfactory; however, no method should be employed indiscriminately. For example, the described calorimeter required a first-order function of time and temperature to describe the extrinsic variation.

In lieu of an examination of each calorimetric experiment, it is recommended that a first-order function of time and temperature be used routinely to characterize a system's extrinsic variation. If either variable in this expression is insignificant, the function automatically reduces to one of those previously described.

The digital transformation (first-derivative approximation) method outlined in this paper has some benefits that support its use in conjunction with the chosen function for the extrinsic variation: (*a*) easy identification of the extrinsic periods, (*b*) compatibility with extrinsic variation functions because the data are in the form necessary to employ linear regression analysis of the actual data, and (*c*) computational procedures that are easily programmable.

Of course, greater confidence is associated with the results when a rigorous approach is used to describe the system. In this case, the proposed method actually permits the investigation of many processes with small thermal effects that may require a relatively long time to reach completion.

REFERENCES

(1) J. J. Chessick and A. C. Zettlemoyer, *Adv. Cat.*, **XI**, 263 (1959).

(2) H. Matsumaru, *Pharm. Soc. Jpn.*, **79**, 63 (1959).

(3) *Ibid.*, **79**, 64 (1959).

(4) H. Nogami, J. Hasegawa, and Y. Nakai, *Chem. Pharm. Bull.*, **7**, 331 (1959).

(5) *Ibid.*, **7**, 337 (1959).

(6) Y. Nakai and Y. Kubo, *Chem. Pharm. Bull.*, **8**, 634 (1960).

(7) Y. Nakai, *ibid.*, **8**, 641 (1960).

(8) J. M. Sturtevant, in "Physical Methods of Organic Chemistry," vol. 1, A. Weissberger, Ed., Interscience, New York, N.Y., 1945, pp. 335–344.

ACKNOWLEDGMENTS

Supported in part by a Biomedical Research Grant, National Institutes of Health.

The authors acknowledge the technical assistance of Mr. T. McDaniels throughout the design, construction, and modification of the calorimeter.

R. G. Hollenbeck is an American Foundation for Pharmaceutical Education Fellow.